Transportation Research Part C 99 (2019) 1–18

Contents lists available at ScienceDirect

Transportation Research Part C

journal homepage: www.elsevier.com/locate/trc

Maximum coverage capacitated facility location problem with range constrained drones

Darshan Chauhan, Avinash Unnikrishnan*, Miguel Figliozzi

Department of Civil and Environmental Engineering, Portland State University, OR 97201, United States

ARTICLE INFO

Keywords:
UAV
Drones
Maximum coverage facility location
Greedy and decomposition heuristics
Energy
Range and capacity constraints

ABSTRACT

Given a set of demand and potential facility locations and a set of fully available charged drones, an agency seeks to locate a pre-specified number of capacitated facilities and assign drones to the located facilities to serve the demands. The facilities serve as drone launching sites for distributing the resources. Each drone makes several one-to-one trips from the facility location to the demand points and back until the battery range is met. The planning period is short-term and therefore the recharging of drone batteries is not considered. This paper presents an integer linear programming formulation with the objective of maximizing coverage while explicitly incorporating the drone energy consumption and range constraints. The new formulation is called the Maximum Coverage Facility Location Problem with Drones or simply MCFLPD. The MCFLPD is a complex problem and even for relatively small problem sizes a state of the art MIP solver may require unacceptably long running times to find feasible solutions. Computational efficiency of MCFLPD solutions is a key factor since conditions associated with customer demands or weather conditions (e.g., wind direction and speed) may change suddenly and require a fast global re-optimization. To better balance solution quality and running times novel greedy and three-stage heuristics (3SH) are developed. The 3SH is based on decomposition and local exchange principles and involves a facility location and allocation problem, multiple knapsack subproblems, and a final local random search stage. On average the 3SH solutions are within 5% of the best Gurobi solutions but at a small fraction of the running time. Multiple scenarios are run to highlight the importance of changes in drone battery capabilities on coverage.

1. Introduction

Several companies like Amazon, Google, UPS, and Flytrex are evaluating the potential use of Unmanned Aerial Vehicles (UAVs) or drones for commercial service or package deliveries (Mack, 2018). Drones are not restricted by the availability of existing infrastructure and therefore can lead to improved last-mile efficiency, safety, and reliability (DHL, 2014). Drones are particularly suitable for emergency applications like search and rescue (Karaca et al., 2018), deliveries of critical medical supplies post-disaster or for emergency response (Thiels et al., 2015; Scott and Scott, 2018), and crop irrigation and pesticide spraying (Albornoz and Giraldo, 2017; Berner and Chojnacki, 2017; Burema and Filin, 2016; Wang et al., 2016; Giles et al., 2016; Faiçal et al., 2014; Costa et al., 2012). Advances in drone technologies regarding lighter and stronger materials for frames (Hassanalian and Abdelkefi, 2017), sensing and coordinating algorithms (Yanmaz et al., 2018, 2017), battery capacity (Li et al., 2017; Fehrenbacher, 2018) and a predictable regulatory framework (FAA, 2018b) are expected to accelerate large-scale UAV adoption. However, a key challenge to

* Corresponding author.
E-mail addresses: drc9@pdx.edu (D. Chauhan), uavinash@pdx.edu (A. Unnikrishnan), mafiglio@pdx.edu (M. Figliozzi).

https://doi.org/10.1016/j.trc.2018.12.001
Received 30 May 2018; Received in revised form 5 December 2018; Accepted 8 December 2018
Available online 03 January 2019
0968-090X/

drone deliveries is their limited range and payload.

Drones have significantly smaller payload carrying capacities and ranges compared to trucks. A diesel cargo van RAM Pro Master 2500 has 378 times the carrying capacity and nearly 20 times the range of a typical drone (Figliozzi, 2017). Moreover, the maximum range of the drone decreases as payload increases. When delivery locations are distributed across a region (urban or rural) trucks can usually cover all demand points from one depot. However, due to its limited range, a drone-based delivery system requires more depots or launching sites distributed across the region. Also, unexpected and/or adverse weather conditions, e.g., headwinds, may dramatically alter the energy consumption and/or range of a delivery drone. Hence, computational efficiency is vital when analyzing drone delivery systems since conditions associated with customer demands and/or weather conditions (e.g. wind direction and speed) may change suddenly and require a fast global reoptimization. A contribution of this research is a novel integer programming model to locate drone launching facilities to meet the demands of spatially distributed customers. This model is called the Maximum Coverage Facility Location Problem with Drones (MCFLPD) and comprises the following: (i) selection of a pre-specified number of capacitated facilities from a list of potential facility locations as drone launching sites, (ii) distribution of a limited number of drones to the selected facilities, (iii) assignment of demand locations to open facilities and drones while respecting the capacity of the facility and the range constraints of the drones.

One of the motivations behind the choice of coverage objective is to evaluate the feasibility of using drones to deliver medical supplies such as defibrillators (Boutilier et al., 2017; Claesson et al., 2017), blood deliveries (Amukele et al., 2017) or critical relief after extreme natural events (Anaya-Arenas et al., 2014; Holguín-Veras et al., 2012; Ozdamar, 2011) while accounting for drone battery range limitations. To better balance solution quality and running times novel greedy and a three-stage heuristics (3SH) are developed. The 3SH is based on decomposition and local exchange principles and involves a facility location and allocation problem, multiple knapsack subproblems, and a final exchange based random search stage.

After a literature review section, the MCFLPD and the proposed solution heuristics are introduced. A real-world case study for making drone deliveries in Portland, OR is presented next. Results concerning solution quality and running times are later presented and discussed. The paper ends with battery sensitivity analyses and conclusions.

2. Literature review

A majority of the research on drone delivery applications have focused on UAV or drone routing and scheduling leading to several interesting variants of the traveling salesman and vehicle routing problems. Murray and Chu (2015) studied the flying sidekick traveling salesman problem (FSTSP) where a drone and a truck deliver in collaboration to a set of customers. The drone takes-off from the truck, makes the delivery, and rendezvous back with the truck at a different location. Murray and Chu (2015) also proposed the parallel drone scheduling traveling salesman problem (PDSTSP) where a set of UAVs and a truck make deliveries from a single depot to customers. Murray and Chu (2015) provide mixed integer linear programming formulations and a route and reassign heuristic for solving the FSTSP and a partitioning heuristics for solving the PDSTSP problem. Ponza (2016) modified the drone delivery time constraints in Murray and Chu (2015)'s FSTSP formulation and developed a simulated annealing metaheuristic. Agatz et al. (2018) denoted the FSTSP as Traveling Salesman Problem with Drones (TSPD), provided approximation results comparing TSPD and TSP optimal solution, and developed several route-first cluster second heuristics which vary in the initial tour generation and assignment of drone delivery nodes. Yurek and Ozmutlu (2018) solved the TSPD using a two-stage iterative decomposition approach where truck routes are determined in the first stage, and drone nodes are assigned in the second stage. Ha et al. (2018) focused on the min-cost TSPD variant of Murray and Chu (2015)'s FSTSP and developed a greedy randomized adaptive search procedure which builds TSPD routes from TSP routes. Carlsson and Song (2017) applied a continuous approximation to the FSTSP (denoted as horsefly routing problem in this paper) and proved that the efficiency gain by adding a drone is a function of the square root of the ratio of the drone and truck velocities.

Wang et al. (2017) and Poikonen et al. (2017) developed several worst-case bounds for the vehicle routing problem with drones (VRPD) where several delivery trucks and drones (launched from trucks) are used to satisfy demands. The bounds provide insights on modifying existing solution algorithms for TSP and VRP variants to obtain solutions to VRPD. Daknama and Kraus (2017) found several nested local search heuristics to be more efficient than the greedy drone assignment approach in solving VRPD. Dayarian et al. (2017) studied the vehicle routing with drone resupply problem where a single drone resupplies a delivery truck from a depot and found that the use of drones improved delivery reliability. Dayarian et al. (2017) studied the dynamic and multiple vehicles and drones variant of Murray and Chu (2015)'s PDSTSP. The authors developed an approximate dynamic programming based heuristic decision making policy to spatially partition the customers into those being served by trucks and those being served by drones. The results show that adding drones to truck fleets can reduce fleet size and increase deliveries. *In contrast to the above works, we consider a drone only delivery system and do not consider truck deliveries as this is the case for medical supplies (*Amukele et al., 2017*).*

Dorling et al. (2017) modeled the drone delivery problem as a single depot multi-trip vehicle routing problem and used linear approximations to study the impact of battery and payload weight on energy consumption. The model was solved using a simulated annealing metaheuristic. Optimizing battery weight was found to be critical for system efficiency. Kim et al. (2018) use a robust optimization approach to model the impact of air temperature uncertainty on drone battery capacity and studied the ability of a fleet of drones to visit multiple locations. Choi and Schonfeld (2017) used a continuous approximation approach to understand the factors affecting a fleet of drone delivery systems. The authors found that battery improvements are critical to overall system coverage and drone delivery systems are more effective in areas with higher demand densities. *In this work, we do not model one-to-many deliveries on each route. We assume that the drones make multiple one-to-one deliveries from the depot locations subject to battery range constraints as is the case with current deliveries of blood supplies.*

Recently, several researchers have focused on facility location problems for drone delivery systems that are more closely related to the topic of this research. For example, Chowdhury et al. (2017) used a continuous approximation approach to develop a humanitarian logistics supply chain post-disaster considering both drones and truck deliveries. The objective is to minimize transportation, inventory, and facility location costs. *We adopt a discrete approach with the objective of maximizing coverage*. Golabi et al. (2017) studied the relief distribution center location model post-disaster where edges may or may not have collapsed due to disaster. Inaccessible demand points are served using drones. The objective is to minimize the travel times of demand points to located facilities and travel time from facilities to inaccessible drones. The model was solved using several metaheuristics with genetic algorithm being the most efficient. Pulver and Wei (2018) developed a facility location model to maximize primary and secondary coverage in the context of transporting and delivering medical supplies using drones. Pulver and Wei (2018) do not consider capacity constraints at drone launching sites or energy consumption as a function of payload and distance for each individual delivery. Also, this paper considers range constraint on multiple trips whereas Pulver and Wei (2018) assume that only one trip is made in the planning period by a drone.

Kim et al. (2017) developed a two-stage model for drone-based pickup and deliveries of medical supplies. In the first stage, a set covering problem is solved to establish depot locations. The second stage is a multi-drone vehicle routing problem. Both Pulver and Wei (2018) and Kim et al. (2017) use solvers such as Gurobi and GAMS to solve their models. *This paper considers a single stage formulation for locating capacitated facilities and assigning demand points to drones. This research also models the allocation of a fixed amount of drones to facilities which is not considered in most of the works mentioned above.*

Hong et al. (2018) study a drone recharging facility location problem which can help increase the coverage range of drones for commercial deliveries. The analysis is based on the worst case drone range at maximum payload. The model is solved using a multi-stage heuristic which embeds principles of greedy, exchange, and simulated annealing solution algorithms. Other researchers have focused on comparing drone delivery systems with traditional truck-based deliveries from an emission and sustainability perspective. Goodchild and Toy (2017) conduct a GIS-based simulation analysis and determine that factors such as distance from depot and number of recipients affect the relative CO_2 emissions of UAVs versus trucks. The authors recommend a mixed drone truck delivery system. Figliozzi (2017) uses continuous approximation techniques and derive analytical formulas to compare operational and lifecycle emissions and energy consumptions of UAVs with conventional diesel, electric vans, and tricycle delivery services. Figliozzi (2017) shows that the delivery strategy (grouping of customers in a route) affects the relative CO_2 emission efficiencies.

A substantial amount of literature exists on the maximum covering facility location problem (MCFLP) (Church and ReVelle, 1974). Farahani et al. (2012) and Daskin (2011) provide excellent reviews of different variants of MCFLP and associated solution strategies. *The MCFLPD model considered in this work is a more complicated variant of MCFLP as the coverage is a function of the drone range which in turns depends on drone availability as well as the payload.* The MCFLPD model also has similarities with the Capacity and Distance Constrained Plant Location Problem (Albareda-Sambola et al., 2009). While Albareda-Sambola et al. (2009) focus on minimizing cost, the model presented in this work focuses on maximizing coverage. *We also explicitly model the distance range constraints resulting from the interaction between battery capacity and the demand carried in a trip. Also,* Albareda-Sambola et al. (2009) *assume a pre-specified number of trucks are available to each open facility whereas, in our model, we assume that a pre-specified number of drones are available to the entire system. The additional drone allocation feature adds to the complexity of the formulation.*

Otto et al. (2018) provide a detailed review of all optimization based papers on civil applications of drones and UAVs. To the best of the authors' knowledge, the MCFLPD model studied in this paper is a novel contribution and the first research to explicitly include drone energy consumption as a function of payload and distance within a drone maximum coverage location problem framework. The solution approaches, the case study, and the sensitivity analysis are also novel contributions.

3. Problem formulation

This section presents the integer linear formulation for the MCFLPD. At the beginning of the planning period, an agency is given a set of demand locations I each having demand w_i, a set of potential facility locations J, and set of available fully-charged drones K. The planning period or time period of analysis is short-term and will depend on the application (for delivery of blood supplies post-earthquake maybe six hours; for delivery of medicine/food in case of an earthquake maybe one day). The agency's goal is to locate p facilities to maximize the demand served. The agency will allocate resource of mass U to each located facility representing the maximum amount of demand which can be served by each located facility in a planning period. U can be viewed as the capacity of the facility. The capacity of a facility corresponds to the maximum amount of demand which can be served from that facility in a period of time. The limiting factor for the capacity in practice would arise from the maximum mass of resources which can be stored at each facility, equipment and building characteristics, staffing levels, etc. The agency will also assign drones to each open facility. The facilities serve as drone launching sites for distributing the resources while respecting the facility capacity and drone range constraints. In this paper, as typical in location problems, we do not consider the cost of transportation of packages and drones from warehouses to these locations. We assume that this cost is a constant irrespective of the configuration of the located facilities. For example, in the event of a disaster, the resources as well as drones can be airlifted to each open facility at the beginning of the planning period. We also assume that the demand during each planning horizon is smaller than the capacity of each drone. If the demand at a location is higher than the drone carrying capacity, that specific node is split into multiple nodes whose demands are less than the drone carrying capacity. Similar assumptions have been made in the drone vehicle routing problem literature (Dorling et al., 2017). Each drone makes several one-to-one trips (facility location to demand point and back) until the battery range B is met as shown in Fig. 1. We do not model one-to-many deliveries which require vehicle routing. This is consistent with initial applications of drone deliveries by companies such as Amazon which is focusing on single package deliveries (Amazon, 2018). As we are looking at a

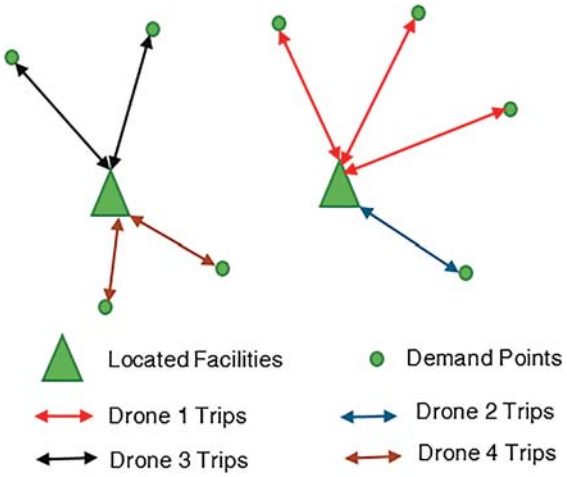

Fig. 1. Schematic representation of the drone delivery system.

relatively small time frame, we do not consider recharging of drone batteries during the planning period. We assume that the drone batteries are recharged overnight or in-between planning periods. The notation used in the formulation is given below.

Fig. 2 shows the demand and potential facility locations used in the case study.

Nomenclature

Sets

I	Set of all demand locations
J	Set of all potential facility locations
K	Set of available drones

Indices

$i \in I$	–
$j \in J$	–
$k \in K$	–

Parameters

η	Power transfer efficiency
θ_s	Lift to drag ratio
B	Battery capacity of each drone
b_{ij}	Battery consumed during one trip between demand $i \in I$ and facility $j \in J$
d_{ij}	Travel distance between demand point $i \in I$ and facility $j \in J$
m_b	UAV battery mass
m_t	UAV mass tare, without battery and load
p	Maximum number of facilities
U	Capacity of each located facility (same unit as UAV mass tare and battery mass)
w_i	Demand for resource at location $i \in I$ (same unit as UAV mass tare and battery mass)

Decision variables

x_{ijk}	1, if customer i is served by the k^{th} drone of plant $j \in J$, and 0, otherwise
y_j	1, if the facility is located at $j \in J$, and 0, otherwise
z_{jk}	1, if the k^{th} drone is assigned to facility $j \in J$, and 0, otherwise

$$\max \sum_{i\in I}\sum_{j\in J}\sum_{k\in K} w_i x_{ijk} \tag{1}$$

$$\sum_{j\in J}\sum_{k\in K} x_{ijk} \leqslant 1, \quad \forall\, i \in I \tag{2}$$

$$\sum_{j\in J} y_j \leqslant p \tag{3}$$

$$\sum_{i\in I} b_{ij} x_{ijk} \leqslant B z_{jk}, \quad \forall\, j \in J,\ k \in K \tag{4}$$

$$\sum_{i \in I} \sum_{k \in K} w_i x_{ijk} \leqslant U y_j, \quad \forall\, j \in J \tag{5}$$

$$z_{jk} \leqslant y_j, \quad \forall\, j \in J,\ k \in K \tag{6}$$

$$\sum_{j \in J} z_{jk} \leqslant 1, \quad \forall\, k \in K \tag{7}$$

$$x_{ijk}, y_j, z_{jk} \in \{0, 1\}, \quad \forall\, i \in I,\ j \in J,\ k \in K \tag{8}$$

The objective (1) is to maximize the demand served. Constraint (2) ensures that each demand location is covered at most once. Eq. (3) restricts the number of facilities located to be less than or equal to p. Constraint (4) enforces battery range constraints on all the drones. Constraint (5) forces the demand served by each located facility to be less than or equal to the capacity of the facility. Constraint (6) ensures that vehicles are assigned only to located facilities. Constraint (7) ensures that each drone is assigned to at most one open facility. Constraint (8) corresponds to variable definition constraints and forces all decision variables to be binary.

The total power consumed in a delivery from facility $j \in J$ to demand point $i \in I$ is given as follows Figliozzi (2017):

$$b_{ij} = \frac{m_t + m_b + w_i}{\theta_s \eta} d_{ij} + \frac{m_t + m_b}{\theta_s \eta} d_{ji} \quad \forall\, i \in I,\ j \in J$$

In this manuscript, we do not consider the impact of charging cycles and weather (wind and temperature) on drone battery capacity. We assume that B is a point estimate which accounts for the above factors. The uncertainty associated with the daily capacity will be considered in a future work. Traditional capacitated facility location models consider location of facilities and allocation of demand points to located facilities. Joint location routing problems consider location of facilities, allocation of demand points to located facilities, and allocation of demand points to vehicle routes with multiple deliveries per route. The model studied in this paper, MCFLPD, is a new type of facility location model. In addition to the location allocation feature of traditional facility location problems, MCFLPD has drone to facility and demand to drone allocation feature while accounting for drone range restrictions. The combination of all of these features makes it a computationally complex problem to solve. The MCFLPD is a more complicated version of the maximum coverage capacitated facility location model which is an NP-Hard problem (Church and ReVelle, 1974; Daskin, 2011).

Traditionally, facility location decisions are long-term strategic decisions and therefore, computational performance is not that important. However, in this paper, the location decision is operational in nature. At the beginning of the time period (which is short-term like a day), an agency will know the demand patterns, weather conditions, etc. and take decisions on where to open facilities (locate a pre-specified number of fully charged drones and resources of mass U) and use the drones to deliver the resources to the demand points. During the next time period, if the weather conditions and demand patterns are similar, then we can use the same solution. Otherwise, we will have to reoptimize the system quickly and potentially open new facilities and relocate the drones. For this purpose, we have developed two heuristics which are described next.

4. Solution approach

This section presents two solution techniques to solve the MCFLPD problem - greedy and three-stage heuristic (3SH). The MCFLPD problem has an inherent complex knapsack structure for which greedy heuristics have been found to be efficient (Loulou and Michaelides, 1979; Goundan and Schulz, 2007; Kang and Park, 2003; Puchinger and Raidl, 2007). We hypothesized that greedy heuristic might be effective for tackling MCFLPD which belongs to the same family. The second solution procedure we developed was a decomposition based three-stage heuristic (3SH). Decomposition heuristics have been found to be useful for problems of this nature in the literature review (Kim et al., 2017; Yurek and Ozmutlu, 2018; Hong et al., 2018) and in traditional location routing problems (Wu et al., 2002; Melo et al., 2009). The final step of the 3SH procedure involves a local exchange heuristic which has been found to be efficient for complex facility location problem variants (Halper et al., 2015). We did explore different Lagrangian Relaxations by dualizing combinations of capacity, allocation, and drone range constraints. However, the bounds obtained were weak and we did not further pursue this direction. Similar insights regarding weak Lagrangian Relaxation bounds were found by Halper et al. (2015) in the context of mobile facility location problem.

4.1. Greedy heuristic

The greedy heuristic has the following steps: (i) creating and sorting a weight matrix, (ii) demand allocation to open facilities, (iii) drone allocation to open facilities, and (iv) demand assignment to drones. Let δ_{ij} be an indicator variable which takes value 1 if demand point i is assigned to open facility j and 0 otherwise. The δ_{ij} variable is initialized to 0 for all demand points and potential facility locations.

Weight Matrix: A weight matrix wt_{ij}, is calculated as:

$$wt_{ij} = \begin{cases} \frac{w_i}{b_{ij}} & \text{if } b_{ij} \leqslant B \\ 0 & \text{otherwise} \end{cases} \quad \forall\ i \in I,\ j \in J \tag{9}$$

A demand and facility location pair with larger weights will have a higher chance of being assigned to each other. The weights are then sorted in non-increasing order and stored in a weight array. Each element in the weight array will have a demand location i and

a potential facility location j associated with it. The sorted weight array is traversed sequentially, and the following demand allocation procedures are applied to each entry.

Demand Allocation: If demand i is already assigned to an open facility, move to the next entry in the sorted weight array. If the demand i is not assigned to any open facility, check if the associated facility j is open. If facility j is open, set $\delta_{ij} = 1$ as long as $wt_{ij} > 0$ and there is residual capacity available in facility j to serve d_i. If facility j is not open, open facility j if the number of facilities currently open is less than p and $wt_{ij} > 0$ and set $\delta_{ij} = 1$. If facility j is not open and if we have already located p facilities then identify a facility j' among the set of open facilities which has the lowest $b_{ij'}$ and available capacity and set $\delta_{ij'} = 1$. If we are unable to assign demand i to an open facility, move to the next element of the sorted weight array. Continue the demand allocation procedure until all the elements of the sorted weight array with positive weights have been processed.

Drone Allocation: Let $\hat{J}$ denote the set of all open facilities. The number of drones required to serve all demands assigned is calculated for each open facility, ND_j, as:

$$ND_j = \left\lceil \sum_{i \in I} \frac{b_{ij}\delta_{ij}}{B} \right\rceil \quad \forall \ j \in \hat{J}$$

Let $\hat{J}_o$ represent the open facilities sorted in non-increasing order of ND_j. Traverse the set $\hat{J}_o$ and assign one drone to each open facility sequentially. In the first round, p drones will be assigned. After assigning one drone to all open facilities, go back to the first facility in $\hat{J}_o$ and continue assigning one drone to each facility sequentially. If the number of drones assigned to a facility is equal to the number of drones required ND_j, then delete that facility from $\hat{J}_o$ and continue the drone assignment. Stop the process when all drones are assigned to open facilities or when the drone requirements of all facilities are met.

Demand to Drone Assignment: For each facility, sort the demand locations in non-decreasing order of battery consumption. Traverse the sorted demand array sequentially and assign demand locations to the first drone as long as the constraints (determined by battery consumption) are not violated. Assign the first demand location which violated the drone range constraint of the first drone to the second drone and continue assigning demands (if the facility has a second drone assigned to it). Repeat until all demands associated with that facility are assigned to drones or until it is not possible to assign any more demands to the final drone for that facility without violating the drone range constraint. Repeat the process for all facilities.

The demand coverage can be calculated by adding the demands for all locations which have been served. The greedy heuristic will ensure the facility capacity and drone range constraints are met.

4.2. Three Stage Heuristic (3SH)

The 3SH heuristic solves the problem in three steps. In the first stage, we solve a facility location problem and determine the facilities to be located and the demand points to be assigned to each facility. In the second stage, knapsack problems are solved to assign drones to facilities and demand points to drones. In the third stage, an exchange heuristic is applied to improve the solution.

4.2.1. Facility location and allocation

The following facility location allocation problem is solved to determine the facilities to be located. Let $\overline{J}_i$ denote the set of potential facility locations which are within the range of the drone for each demand location i, i.e., $\overline{J}_i = \{j: b_{ij} \leqslant B\}$. The decision variables for this optimization formulation are: (i) $\hat{x}_{ij}$ which takes value 1 if demand $i \in I$ is assigned to facility $j \in J$ and 0 otherwise, and (ii) $\hat{y}_j$ which takes value 1 if the facility j is located and 0 otherwise.

$$\max \quad \sum_{i \in I} \sum_{j \in \overline{J}_i} \frac{w_i}{b_{ij}} \hat{x}_{ij} \tag{10}$$

$$\sum_{j \in \overline{J}_i} \hat{x}_{ij} \leqslant 1, \quad \forall \ i \in I \tag{11}$$

$$\sum_{j \in J} \hat{y}_j \leqslant p \tag{12}$$

$$\sum_{i \in I} w_i \hat{x}_{ij} \leqslant U, \quad \forall \ j \in \overline{J}_i \tag{13}$$

$$\hat{x}_{ij} \leqslant \hat{y}_j, \quad \forall \ i \in I, \ j \in \overline{J}_i \tag{14}$$

$$\hat{x}_{ij}, \hat{y}_j \in \{0, 1\}, \quad \forall \ i \in I, \ j \in \overline{J}_i \tag{15}$$

Constraint (11) ensures that each demand point is assigned to at most one of the facilities within flying range. Constraint (12) enforces that at most p facilities are located. Eq. (13) ensures that the sum of demand assigned to a facility is less than the facility capacity. Constraint (14) makes sure that each demand point is assigned to located facility only. The objective function maximizes the weight of assigning demand points to facilities where the weight is defined in Eq. (9). The above formulation is similar to a capacitated p-median facility location problem (Daskin, 2011).

4.2.2. Repeated application of knapsack problems

Let $\hat{J}$ and $\hat{I}_j$ denote the set of facilities located and the set of demand locations assigned to each open facility obtained at the end of the facility location and allocation stage. Note that $\hat{J} = \{j \in J: \hat{y}_j = 1\}$ and $\hat{I}_j = \{i: \hat{x}_{ij} = 1\}$. In the second step, we assign drones to facilities and demand locations to drones by repeatedly solving the maximum profit knapsack problem. For any open facility $j \in \hat{J}$ and drone $k \in K$, the maximum profit knapsack problem can be defined as follows:

$$C_j = \max \quad \sum_{i \in \hat{I}_j} w_i x_i' \tag{16}$$

$$\sum_{i \in \hat{I}_j} b_{ij} x_i' \leqslant B \tag{17}$$

$$x_i' \in \{0, 1\} \tag{18}$$

In the above formulation, the decision variable is x_i' which takes value 1 if demand i is served by a drone and 0 otherwise. C_j denotes the optimal objective function (16) value which corresponds to the maximum demand which can be served by a drone at a facility j from the set of demand locations $\hat{I}_j$. Constraint (17) ensures that the demand points assigned to a drone are within the battery range, i.e., a drone can make one-to-one deliveries to all the assigned demand points without exhausting the battery capacity. The steps of the second stage of 3SH are described below.

- Solve p maximum profit knapsack problem, one for each facility in $\hat{J}$. Let j' denote the facility with the maximum value of C_j, $\forall\, j \in \hat{J}$. Assign the first drone to facility j'. Assign the demand locations in $\hat{I}_{j'}$ with $x_i' = 1$ to the first drone. Update $\hat{I}_{j'}$ by removing all demand points which have been assigned to the drone.
- Solve the maximum profit knapsack problem for facility j' with the new set of demand points $\hat{I}_{j'}$. Update the value of $C_{j'}$. Compare the p knapsack objectives and determine the facility with a maximum value of C_j. Let j'' denote the facility with the highest knapsack objective. Assign the second drone to facility j''. Assign the demand points in $\hat{I}_{j''}$ with $x_i' = 1$ to the second drone. Update $\hat{I}_{j''}$ by removing all demand points which have been assigned to the drone.
- Repeat the above steps until all drones or all demand points have been assigned. The number of repetitions will be at most $|K| - 1$. Now we can determine the coverage by adding the demand of all points which have been served.

The second stage involves solving at most $p + |K| - 1$ maximum profit knapsack problems in total.

4.2.3. r-exchange heuristic

In the third stage, we employ a local exchange heuristic to improve the solution. First, set $\hat{J}_0 = \hat{J}$ and determine the total demand served by each facility. The r lowest demand facilities are identified and removed from the set $\hat{J}$. The set of open facilities $\hat{J}$ is then updated with r facilities which are randomly picked from the remaining $|J| - p + r$ facility locations. Update the $\overline{J}_i = \{j \in \hat{J}: b_{ij} \leqslant B\}$. Now that we have fixed the open facilities and identified the facilities which can serve each demand location based on the drone range, the following allocation problem is solved. The allocation formulation shown below, Eqs. (19)–(23), is almost the same as formulation (10)–(15) with one difference. In the formulation shown below $\hat{y}_j = 1 \;\; \forall\, j \in \hat{J}$ and 0 otherwise and is not a decision variable. The decision variables are $\hat{x}_{ij}$ which take value 1 if demand $i \in I$ is assigned to facility $j \in \overline{J}_i$ and 0 otherwise.

$$\max \quad \sum_{i \in I} \sum_{j \in \overline{J}_i} \frac{w_i}{b_{ij}} \hat{x}_{ij} \tag{19}$$

$$\sum_{j \in \overline{J}_i} \hat{x}_{ij} \leqslant 1, \quad \forall\, i \in I \tag{20}$$

$$\sum_{i \in I} w_i \hat{x}_{ij} \leqslant U, \quad \forall\, j \in \overline{J}_i \tag{21}$$

$$\hat{x}_{ij} \leqslant \hat{y}_j, \quad \forall\, i \in I,\; j \in \overline{J}_i \tag{22}$$

$$\hat{x}_{ij} \in \{0, 1\}, \quad \forall\, i \in I,\; j \in \overline{J}_i \tag{23}$$

Once the allocation problem is solved, the second stage is repeated by solving $p + |K| - 1$ max profit knapsack problems. If there was an increase in the total demand served, the current best solution is recorded and $\hat{J}_0$ is updated to be the new set of open facilities $\hat{J}$. If there was no improvement, the current best solution corresponds to the total demand served by the open facilities $\hat{J}_0$ and a new set of r facilities is randomly chosen. This exchange heuristic is run a pre-specified number of times.

5. Numerical analysis

The feasibility of using drones for deliveries is tested on a Portland Metropolitan Area case study. The centroids of ZIP Code Tabulated Areas (ZCTAs) in the Portland Metro Region are selected as the demand locations for the case study. There are a total of 122 demand locations. The community centers throughout the Portland Metro Area are selected as the potential facility locations

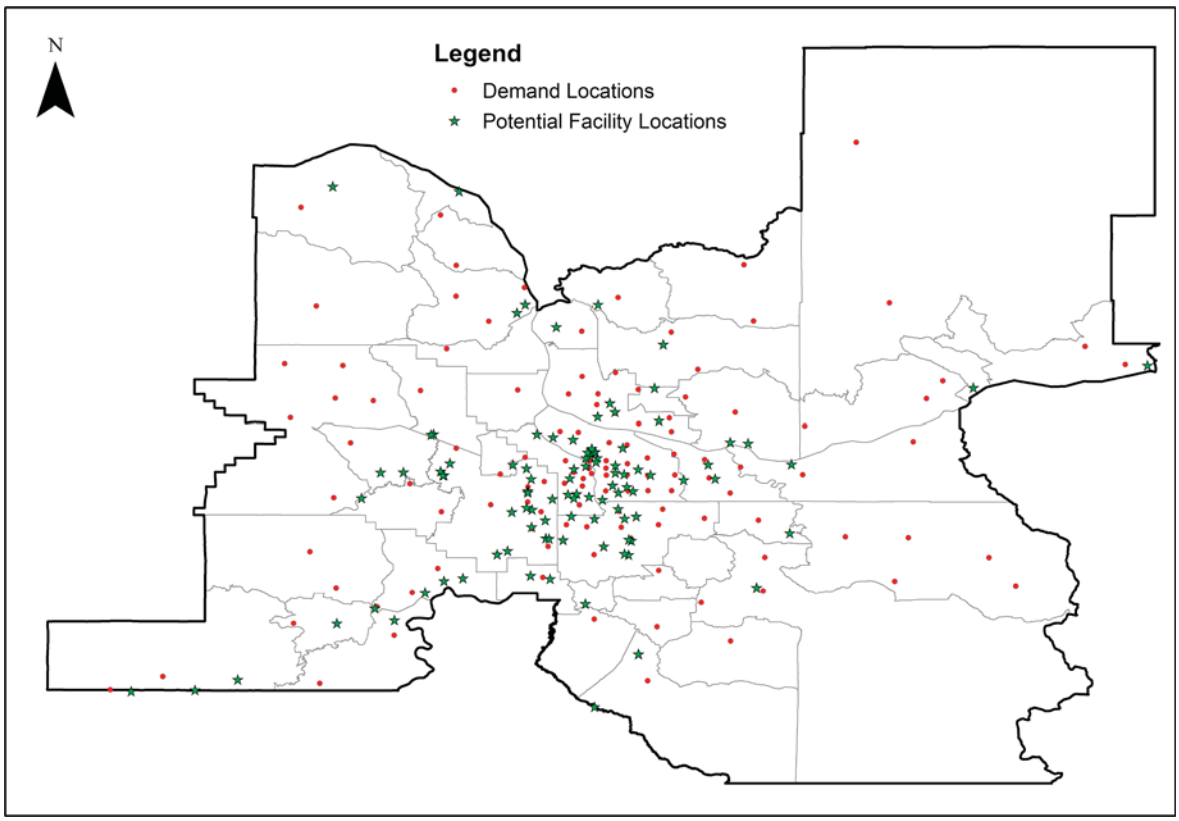

Fig. 2. Demand and potential facility locations in the Portland Metropolitan Region.

(refer Appendix A). In our study, the facilities should have adequate space for launching drones as well as storing the resources which are supplied. Community centers in Portland Metropolitan Area satisfy both criterions and are public facilities. There are a total of 104 potential facility locations in the case study. The demand locations and potential facility location do not overlap. Fig. 2 shows the demand and potential facility locations used in the case study.

The 122 payloads to be delivered at customer demand points are randomly generated from a discrete uniform distribution ranging from 1 kg to 5 kg at intervals of 0.25 kg (refer Appendix A). The sum of all demands is 366.5 kg. The capacities of each facility U are generated as in Pirkul and Schilling (1989) as shown below:

$$U = \frac{\sum_{i \in I} w_i}{0.8p}$$

In the above equation, the numerator represents the total demand to be satisfied, and p denotes the number of facilities to be located. In this study, the number of facilities to be located varies from 5 to 30 in multiples of 5. The travel distance between the demand and potential facility location is taken to be the Euclidian distance, as drones typically travel in straight lines between two points. We do not consider the impact of obstacles such as mountains or tall buildings or “no drone zones”(FAA, 2018a) in this case study. This can be a potential future extension. The following parameters are assumed for the drones unless specified otherwise (Figliozzi, 2017):

- Power transfer efficiency (η) 0.66
- Lift to drag ratio (θ_s) 3.5
- Tare weight 10.1 kg
- Maximum payload 5 kg
- Battery capacity 777 W h
- Battery safety factor 1.25 (80% of Maximum Battery Capacity)

All computational runs are conducted on a Windows 10 desktop with Intel Core i7-7700 CPU 3.6 GHz, 4 Core(s), 8 Logical Processor and 32 GB of RAM.

Table 1
Comparison of Gurobi solver, Greedy Heuristic, and 3SH.

p	$\|K\|$	Gurobi				Greedy		3SH							
		Time (sec)	Coverage (%)	Gap (%)	Coverage at 1800 sec (%)	Time (sec)	Coverage (%)	Time (sec)				Coverage (%)			
								S2	Ave	Min	Max	S2	Ave	Min	Max
5	20	7200	56.4	2.1	56.3	0.1	45.2	1.1	14.7	14.4	15.0	52.7	54.5	53.6	55.1
5	25	7200	61.9	2.0	61.7	0.1	50.3	1.1	15.9	15.6	16.2	58.3	59.5	58.6	60.2
5	30	7200	66.3	1.9	66.2	0.1	55.3	1.1	16.7	16.4	17.1	62.9	63.7	62.9	64.5
5	35	7200	70.2	1.2	69.5	0.1	58.9	1.2	18.3	17.6	22.8	66.5	67.0	66.5	67.9
5	40	7200	72.7	1.6	72.6	0.1	62.5	1.2	18.8	18.2	19.1	69.0	69.9	69.1	70.5
10	20	7200	64.4	2.5	64.4	0.2	48.2	1.1	16.6	16.1	16.9	59.1	61.4	59.8	62.6
10	30	7200	75	3.1	75	0.2	59.8	1.1	18.3	17.9	19.0	67.9	71.5	70.1	72.9
10	40	7200	83.8	1.7	83.8	0.2	67.1	1.1	20.1	19.2	20.8	70.2	78.4	76.3	80.4
15	30	7200	79.7	3.8	79.2	0.2	59.2	1.0	21.9	21.4	22.7	70.3	75.2	73.2	77.2
15	45	7200	90.2	1.7	89.8	0.2	73.1	1.0	24.3	23.4	25.5	74.4	83.9	80.3	86.6
15	60	7200	92.6	1.3	92.5	0.3	73.1	1.0	24.8	23.6	25.7	74.4	85.0	81.2	88.7
20	20	7200	71.2	2.1	71.1	0.3	52.8	1.0	25.1	24.6	25.6	61.7	65.8	63.2	67.5
20	40	7200	90.4	2.4	89.9	0.3	70.7	1.0	28.7	28.1	29.3	77.5	84.2	82.7	85.3
20	60	320	93.8	0.0	NA	0.3	72.2	1.0	30.4	28.6	31.8	78.9	87.2	83.6	90.1
20	80	36	93.8	0.0	NA	0.4	72.2	1.0	30.9	29.6	32.8	78.9	87.5	83.6	91.3
25	25	7200	79.6	3.5	79.5	0.3	53.6	1.0	33.0	32.1	35.0	67.3	71.5	69.2	73.3
25	50	337	93.8	0.0	NA	0.4	71.4	1.0	36.6	35.7	38.3	80.1	88.9	85.2	92.2
25	75	27	93.8	0.0	NA	0.5	71.4	1.0	37.4	36.2	39.0	80.1	88.2	84.2	91.0
25	100	43	93.8	0.0	NA	0.5	71.4	1.0	38.1	36.9	39.5	80.1	89.5	86.1	92.2
30	30	7200	85.3	4.1	84.2	0.3	60.6	1.0	40.3	39.0	41.7	72.9	76.8	74.4	80.2
30	60	23	93.8	0.0	NA	0.5	74.8	1.0	44.3	43.3	45.5	86.2	90.9	88.7	92.8
30	90	31	93.8	0.0	NA	0.6	74.7	1.0	45.1	44.2	46.4	86.2	90.7	88.7	93.0

NA = Not Applicable.
S2 = After Step 2.

5.1. Computational efficiency

Computational efficiency of MCFLPD solutions is a key factor in real-world implementations. Initial conditions associated to customer demands and/or weather conditions (wind direction and speed) may change suddenly and may require a fast global reoptimization of the MCFLPD with different safety factors (a change in regional weather conditions will affect the energy consumption of all deliveries). A later section describes a sensitivity analysis based on different levels of allowable battery consumption. The Portland Case Study is solved using the following three methods:

- Gurobi solver using the Python interface. The model is run for a maximum of 7200 sec or until a solution is obtained. Default parameters are assumed for the Gurobi Solver.
- Greedy Heuristic which is implemented in Python.
- Three Stage Heuristic (3SH): The facility location allocation problem in stage 1 and knapsack problems in stage 2 are solved using Gurobi. The number of facilities to be exchanged in the third stage is fixed at 2 unless specified otherwise. The exchange heuristic is run for a maximum of 100 iterations.

The first set of computational runs aim at comparing the computational efficiency of the greedy heuristic and 3SH with the Gurobi solver for different maximum number of facilities and drone availabilities (see Table 1). Since the facilities to be exchanged are picked randomly in 3SH, we run 30 instances and report the average, minimum, and maximum computational times as well as coverage results. We limit the number of facilities to be exchanged in the third stage of 3SH to just two. Coverage for the purpose of this paper is defined as the percentage of total demand met.

The greedy heuristic achieves 78.01% value of Gurobi on average (Best: 85.9% of Gurobi solution for $p = 5$, $|K| = 40$; Worst: 67.36% of Gurobi solution $p = 25$, $|K| = 25$). The greedy heuristic provides solutions which are on average within 20% of the best Gurobi solution but takes a maximum computational time of only 0.6 sec. According to the approximation algorithms literature in facility location, greedy and approximate algorithm solutions differ from optimal solutions in the worst case by at least 33% (Shmoys et al., 1997; Jain and Vazirani, 2001). The MCFLPD is a more complex variant of facility location problems. Therefore, we expect the worst case bounds to be weaker. However, we note empirically that all solutions are well within the worst case bounds for facility location problems. Gurobi solver successfully finds optimal solutions as resources become abundant (p increases and maximum

Table 2
Battery energy consumed per unit of coverage.

p	$\|K\|$	Gurobi	Greedy	3SH
5	20	213.9	205.7	213.3
5	25	234.1	224.7	235.1
5	30	259.3	242.7	257.3
5	35	293.4	266.1	285.4
5	40	310.5	291.9	308.2
10	20	183.7	180.9	178.1
10	30	226.3	217.3	227.1
10	40	274.4	268.1	268.4
15	30	213.7	219.3	208.8
15	45	275.8	277.6	258.1
15	60	347.5	277.6	268.7
20	20	158.4	144.0	149.2
20	40	241.7	233.6	225.7
20	60	329.7	250.1	253.3
20	80	386.3	250.1	253.8
25	25	169.7	165.5	152.9
25	50	274.4	249.1	239.7
25	75	372.2	249.1	240.7
25	100	416.3	249.1	242.6
30	30	180.0	174.4	161.1
30	60	309.5	248.2	227.5
30	90	394.2	248.3	230.7

available drones increases). Gurobi finds the true optimal solution, within the 2-h runtime limit, in nearly one-third of the cases all of which have higher than 20 potential facility locations and at least 50 drones.

The average 3SH solutions are nearly 95% of the best Gurobi solutions on average. The best case is when 3SH achieves 96.9% of Gurobi solution for $p = 5$, $|K| = 20$ and $p = 30$, $|K| = 60$. In the worst case, 3SH achieves 90% of Gurobi solution for 25 potential facility locations and 25 maximum number of drones. The 3SH approach is significantly faster than Gurobi; the median reduction in

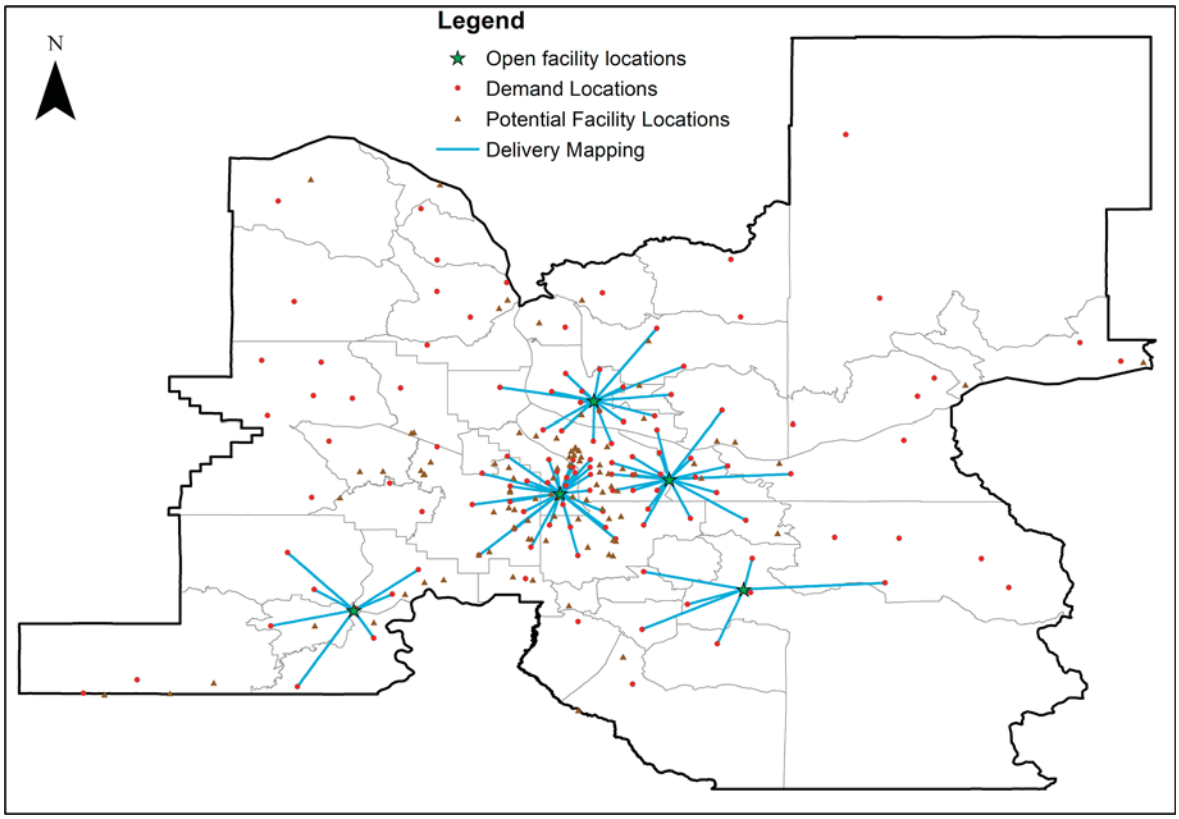

Fig. 3. Case (i): Gurobi solution ($p = 5$ and $|K| = 35$).

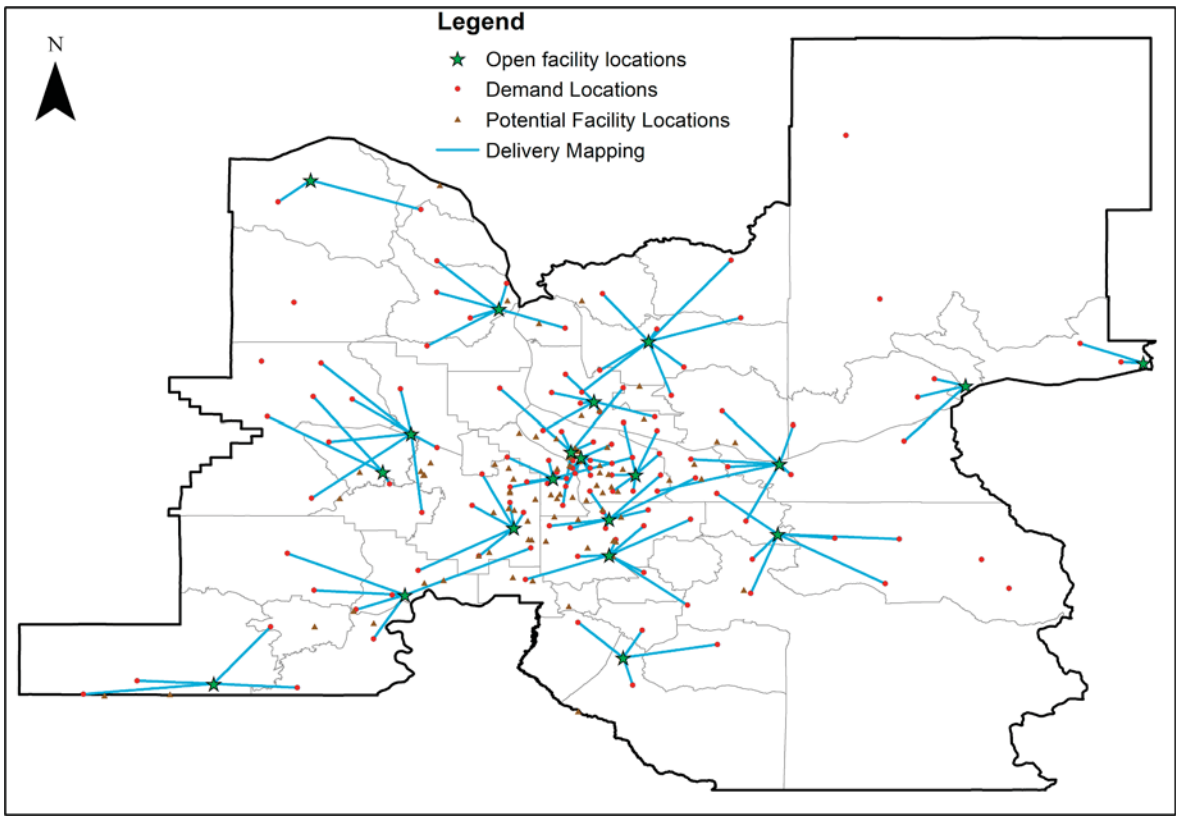

Fig. 4. Case (ii): Gurobi solution ($p = 20$ and $|K| = 60$).

computational time is 99.7%. When the r-exchange heuristic is not run, i.e., the heuristic is stopped after repeated applications of the knapsack problem, the heuristic provides solutions which are on an average within 85.9% of the Gurobi solution with an average computational time of 1.2 sec. The local search step takes an additional 26 sec on average but helps improve the solution by another 9% making it close to the optimal solution.

Table 2 presents the average energy consumed per percent coverage which is calculated as follows:

$$\text{Energy/Coverage} = \frac{\text{Average Battery Used} \times \text{Number of Drones Used}}{\text{Coverage}}$$

Table 2 shows that Gurobi is competitive against 3SH when the number of facilities is less, but starts losing edge when p becomes 15 or greater and progressively worsens against 3SH with an increase in p. The effect is also amplified with an increase in $|K|$, for the same p. This shows that 3SH is much more efficient in terms of drone employment to achieve a similar coverage.

5.2. Coverage analysis

In this section, we analyze one scenario with low coverage and one scenario with high coverage: (i) p = 5 and $|K| = 35$ with an optimal coverage of 70.2%, and (ii) p = 20 and $|K| = 60$ with an optimal coverage of 93.8%. Fig. 3 shows the delivery mapping of Gurobi solution for case (i). The delivery spiders are distinct and do not overlap over one another. The minimum facility utilization is 23.9% of its total capacity, and the maximum facility utilization is 87.8% of its total capacity. These results indicate that drone battery range capacity is constraining the coverage. With five facilities, most of the demand locations around the downtown region are covered which is intuitive as this is the area with the highest density. Coverage is limited in low-density areas, e.g., the Northeast region.

Fig. 4 shows the delivery maps of Gurobi solution with 20 open facility and 60 available UAVs for case (ii). It can also be seen from the figure that the central region has a lot of overlapping spiders, which suggests that facilities have reached their capacity. The maximum facility utilization is 100% and the minimum facility utilization is 39.1% of their total capacity. Fig. 5 visualizes the facilities which have utilized more than 85% of their capacity. Most of the facilities with more than 85% capacity utilization are in the downtown region. The demand points which are not served in this case are beyond the range of the drone from any community center and therefore will require improvements in battery capacity (see Table 3). The battery capacity improvements needed to achieve 100% coverage is studied in Section 5.5. The insights obtained are consistent with (Choi and Schonfeld, 2017) on the increased effectiveness of drone delivery systems in higher demand density regions and Dorling et al. (2017) on the critical nature of batteries.

We also compare the solutions obtained from 3SH and Greedy algorithm with the Gurobi solution. From Figs. 5–7, it can be

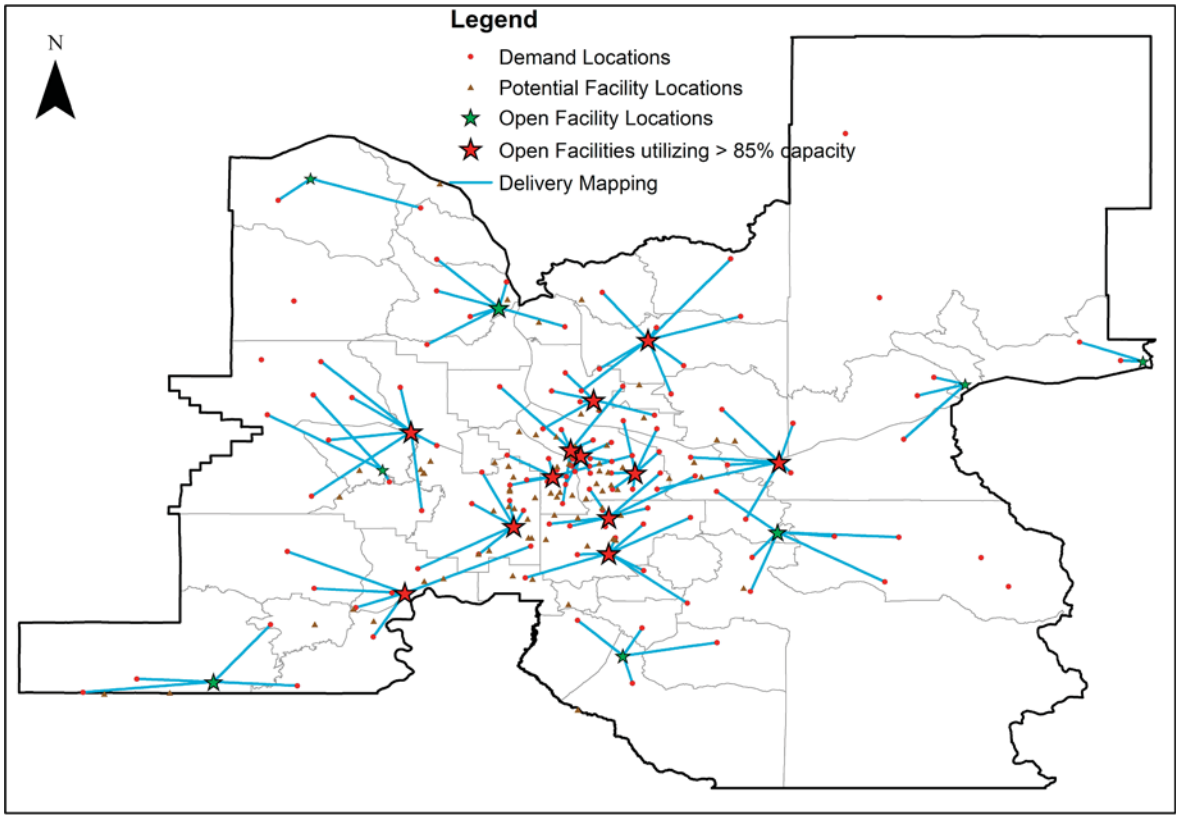

Fig. 5. Case (ii): Gurobi solution highlighting facilities which have greater than 85% utilization ($p = 20$ and $|K| = 60$). Size of star corresponds to facility utilization.

Table 3
Summary of unmet demand points for case (ii).

Unmet demand ZCTA	Closest facility ID	Battery requirement (W h)
97028	56	1118
97049	56	854
97064	23	779
97144	66	750
98610	10	691
98616	2	1624

observed that facilities are more spatially dispersed in the Gurobi solution. The spatial dispersion shrinks a little in the 3SH solution, and then shrinks significantly in the Greedy solution, confined mostly to dense urban areas. The allocation of facilities is based on the weight matrix (Eq. (9)). The higher the weight, the greater the priority a facility gets when the demand allocation takes place. Therefore, if a demand point and a candidate facility location are located close by (resulting in very small values of b_{ij}), the weight is higher. In the central region, the density of both, candidate facility locations and demand points, is much higher. This is evident in facility location using the Greedy algorithm (ref. Fig. 6), where a majority of its open facilities are concentrated in the central region. In Figs. 5–7, the size of the stars representing open facilities indicate its capacity usage. It can be observed that the density of facilities in the central region in Gurobi solution is much lesser and also that, all of the facilities opened there have capacity utilization greater than 85%. While, in the Greedy solution the facilities are “boxed-in” the urban core which results in very less capacity utilization of capacities. The capacity utilization in 3SH is much more consistent across facilities compared to Greedy solution. It can also be noticed that the number of facilities utilizing more than 85% of its capacity significantly reduced for 3SH and Greedy in comparison to Gurobi. In spite of this, the 3SH solution provides about 95% coverage of the Gurobi coverage.

5.3. Sensitivity to battery safety factor

In the initial set of experiments, the battery safety factor is set to be 1.25 (drones cannot utilize more than 80% of the battery capacity) to account for weather-related uncertainties, battery usage during take-off and landing, and uncertainties regarding initial

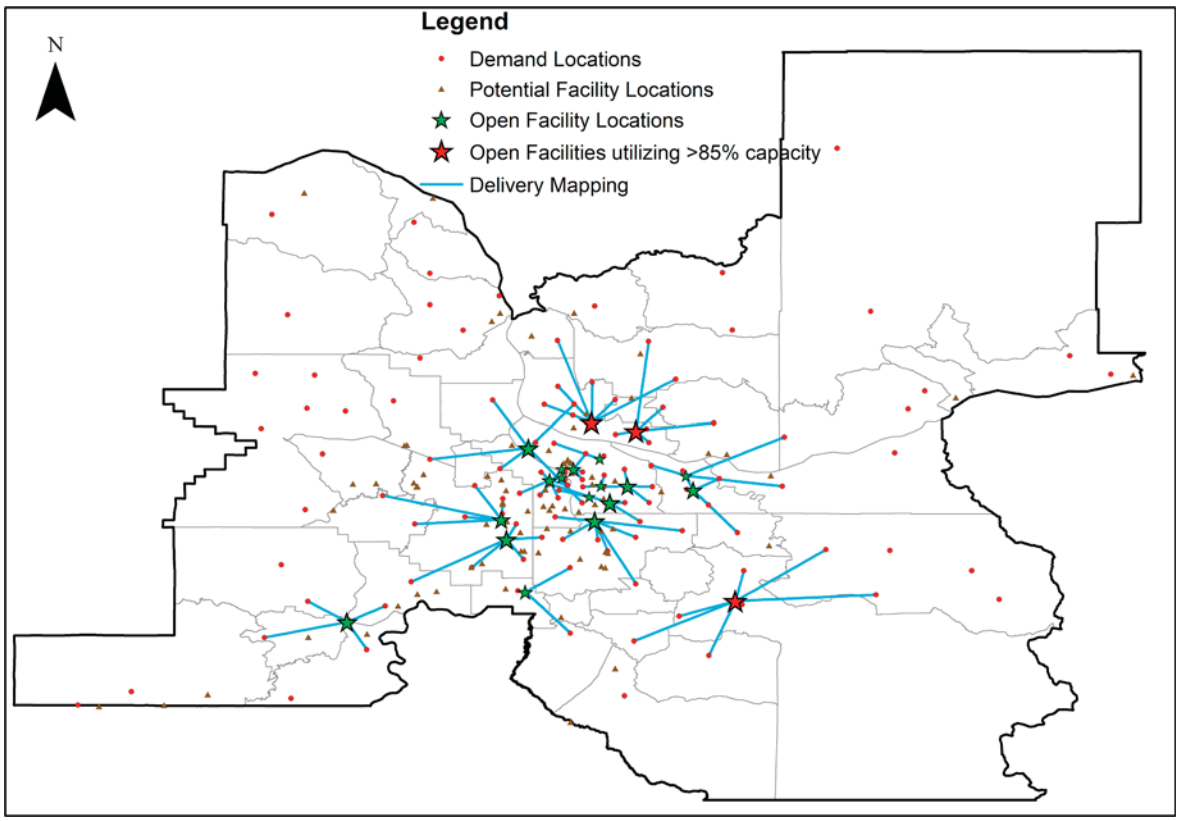

Fig. 6. Greedy solution highlighting facilities which have greater than 85% utilization ($p = 20$ and $|K| = 60$). Size of star corresponds to facility utilization.

battery conditions (Figliozzi, 2017; Microdrones, 2018). The goal of this set of experiments is to study the impact of the variation in battery safety factor on the coverage. The battery safety factor considered in this analysis include safety factors 10/7.0, 10/7.5, 10/8.5, and 10/9.0. These correspond to 70%, 75%, 85%, and 90% of the battery capacity respectively. Table 4 presents the average of percentage deviation of coverage at specified maximum battery utilization (MBU) from the coverage achieved assuming a maximum battery utilization of 80% across 30 runs.

$$\text{Percent Deviation} = \sum_{i=1}^{30} \frac{\text{Coverage}_x^i - \text{Coverage}_{80}^i}{\text{Coverage}_{80}^i} \times 100$$

Coverage_{80}^i represents the coverage at 80% maximum battery utilization and Coverage_x^i is the coverage at x % maximum battery utilization in the i^{th} run of 3SH. In general, the effects of having a high battery safety factor (less available energy) are more profound than the effects of a low battery safety factor (more available energy). As shown in Table 4, the effect of the battery safety factor decreases marginally as p (the number of open facilities) increases.

5.4. Sensitivity to number of facilities to be exchanged in 3SH

In all the runs completed until now, two facilities (two removed and added) were exchanged in the third step of the 3SH heuristic. We now vary the number of facilities to be exchanged and study the variation in computational times and improvement in coverage. The values presented in Table 5 are the average of 30 runs. A 1 facility exchange in 3SH works best when $p = 5$; a 2 facility exchange in 3SH works best when $p = 10$, and a 3 facility exchange in 3SH works best for $p \geqslant 15$. No benefits were found when the number of facilities exchanged was 4 or higher. The runtimes are comparable on average which is expected given that the underlying problem sizes are not significantly altered by the size of the exchange procedure.

5.5. Sensitivity to changes in battery capacity

This section shows how coverage would improve with changes in the battery capacity of the drone. All instances were solved using Gurobi. The ideal scenario portrays the improvement in the battery without an increase in the drone tare weight, which may be possible due to future breakthroughs in the battery technology. The realistic scenario assumes that we can improve the battery

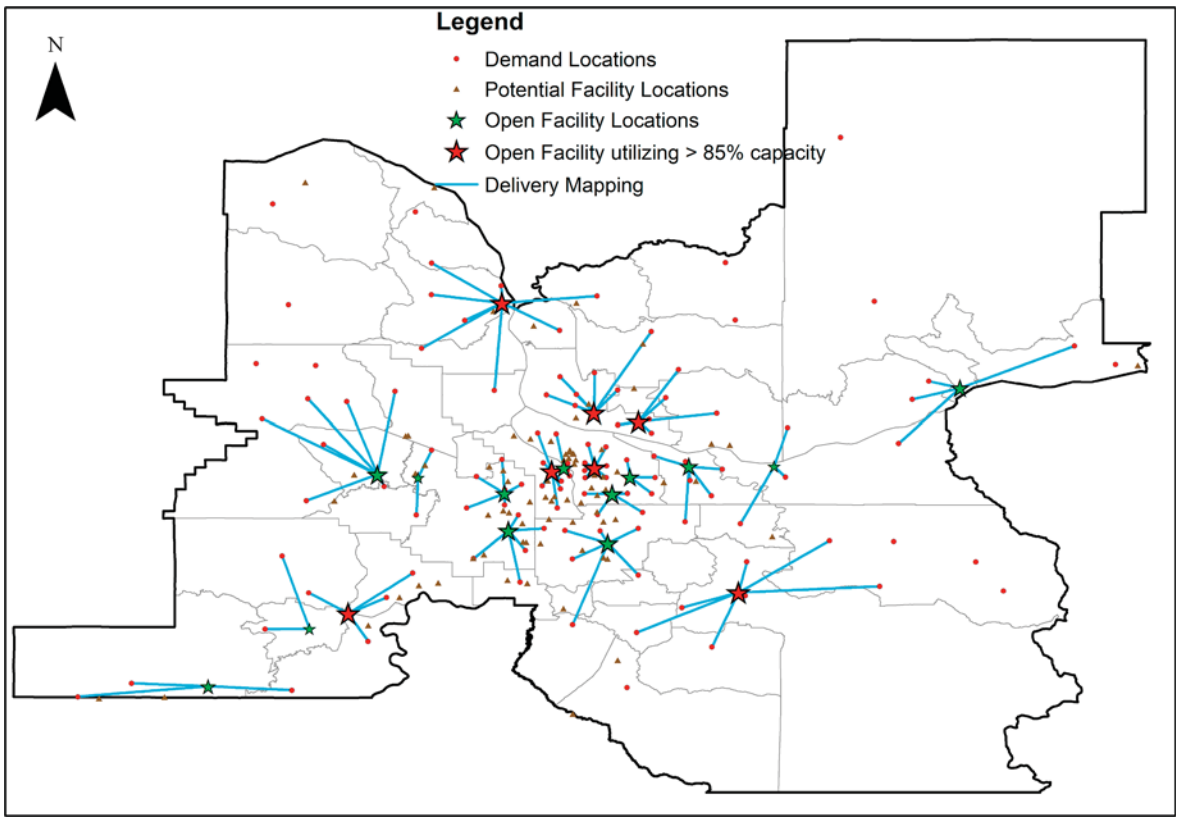

Fig. 7. 3SH solution highlighting facilities which have greater than 85% utilization ($p = 20$ and $|K| = 60$). Size of star corresponds to facility utilization.

Table 4
Variation of percent deviation in average coverage with respect to the average coverage achieved at 80% MBU.

p	Percent deviation with respect to 80% MBU				
	70% MBU	75% MBU	85% MBU	90% MBU	Range
5	−7.5	−3.5	2.1	4.2	11.8
10	−5.9	−3.9	1.7	4.3	10.3
15	−4.8	−2.1	1.8	3.9	8.8
20	−4.5	−2.0	1.8	4.0	8.5
25	−4.2	−1.7	1.1	3.0	7.3
30	−4.0	−2.3	1.4	3.1	7.2

capacity of a drone by adding additional batteries. This results in an increase in drone tare weight which leads to increased battery consumption for the same amount of distance traveled. The UAV/drone in consideration uses Lithium polymer (LiPo) batteries. It is reported that the specific energy of LiPo batteries can go up to 275 W h/kg (Amicell, 2018). So, for the realistic case study, the specific energy is taken to be 255 W h/kg with 80% MBU. The analysis is conducted for the case when $p = 20$, $|K| = 60$. It is observed that about 165% increase in the battery capacity is required to achieve full coverage in the ideal case (see Table 6). In the realistic scenario, this increase is still not sufficient to achieve 100% coverage. This is because, the increase in distance traveled is not as high as in the ideal case due to the additional battery consumption.

An important conclusion from the sensitivity analysis is that runtime increases substantially as battery capacity increases. This is likely the result of additional complexity due to the increase of feasible options that must be analyzed by the MIP solver. *Hence, the value of a high quality and yet computationally efficient heuristic like 3SH is likely to increase substantially in the future.*

6. Conclusions

This paper presents a novel model denoted MCFLPD for coverage-based capacitated facility location problem with drones by factoring in real-life UAV battery and weight constraints. MCFLPD is substantially more complex than traditional capacitated facility location

Table 5
Impact of different number of facilities exchanged in 3SH.

p	$\|K\|$	After Step 2		1 facility exchange		2 facility exchange		3 facility exchange	
		Coverage (%)	Time (sec)	Coverage (%)	Time (sec)	Coverage (%)	Time (sec)	Coverage (%)	Time (sec)
5	20	52.7	1.1	54.4	15.4	54.5	14.7	53.8	13.5
5	25	58.3	1.1	60.0	16.1	59.5	15.9	59.0	14.3
5	30	62.9	1.1	64.5	17.2	63.7	16.7	63.3	15.1
5	35	66.5	1.2	67.8	18.0	67.0	18.3	66.9	15.9
5	40	69.0	1.2	70.4	18.8	69.9	18.8	69.9	16.6
10	20	59.1	1.1	60.8	15.5	61.4	16.6	61.0	15.7
10	30	67.9	1.1	70.4	17.3	71.5	18.3	71.2	17.2
10	40	70.2	1.1	76.7	18.7	78.4	20.1	78.4	18.5
15	30	70.3	1.0	74.2	20.8	75.2	21.9	75.2	20.5
15	45	74.4	1.1	82.2	22.7	83.9	24.3	84.8	22.4
15	60	74.4	1.1	82.4	22.9	85.0	24.8	86.2	22.7
20	20	61.7	1.1	65.7	24.2	65.8	25.1	66.3	23.4
20	40	77.5	1.1	83.6	27.4	84.2	28.7	84.5	26.2
20	60	78.9	1.1	85.0	28.8	87.2	30.4	88.6	27.3
20	80	78.9	1.1	84.9	29.1	87.5	30.9	88.9	27.4
25	25	67.3	1.1	71.1	31.3	71.5	33.0	72.0	29.4
25	50	80.1	1.1	87.8	35.3	88.9	36.6	90.2	32.2
25	75	80.1	1.1	87.0	35.8	88.2	37.4	89.4	32.3
25	100	80.1	1.1	86.6	36.4	89.5	38.1	90.2	32.3
30	30	72.9	1.1	76.9	38.4	76.8	40.3	77.1	34.2
30	60	86.2	1.1	89.5	42.8	90.9	44.3	91.5	37.0
30	90	86.2	1.1	89.3	43.4	90.7	45.1	91.1	37.0

Table 6
Impact of battery capacity on coverage.

Battery	Ideal			Realistic		
	Tare mass	Coverage (%)	Time (sec)	Tare mass	Coverage (%)	Time (sec)
777	10.1	93.8	410	10.1	93.8	410
1032	10.1	96.7	1233	11.1	95.7	667
1287	10.1	97.4	1204	12.1	97.4	978
1542	10.1	98.7	2212	13.1	97.4	873
1797	10.1	98.7	2557	14.1	97.4	1475
2052	10.1	100	2070	15.1	98.7	1377

problems. As real-world drone-based deliveries have already started being implemented in the field, it is necessary to study facility location for drones not only for economic purposes but also for social/humanitarian benefit. Drone deliveries tend to be time-sensitive, e.g. medical supplies, and/or subject to unexpected changes in weather conditions. Hence, solution times are as important as solution quality.

In this research, three solution approaches are presented and compared. A state of the art MIP solver deliver high-quality solutions but requires unacceptably long running times to find feasible solutions reliably. A greedy algorithm is extremely fast, less than one second on average, but at the cost of solution quality (nearly 20% coverage loss). The three-stage heuristics (3SH) is based on decomposition and local exchange principles and on average the 3SH solutions are within 5% of the best Gurobi solutions but require in all cases substantially less running time (at most 46 sec). The 3SH heuristic achieves this balanced performance by leveraging the problem structure to obtain solutions with high coverage but also more economical in terms of drone employment and in an appropriate time.

The sensitivity analysis on the battery safety factors suggests that the effects of increasing battery safety are acute. An analysis to estimate the technological improvement in the battery capacity was also performed. It showed that a breakthrough in battery technology is required to achieve one hundred percent coverage for the case study considered in this work. It was also demonstrated that MIP solver (Gurobi) solution times increase substantially as battery technology increases. This result further enhances the value of an efficient algorithm such as the proposed 3SH heuristic.

Acknowledgements

Co-author Miguel Figliozzi was funded by the Freight Mobility Research Institute (FMRI), a U.S. DOT University Transportation Center.

Appendix A. List of demand points and candidate facility locations

See Tables A.7 and A.8.

Table A.7
List of demand points with assumed demand.

ZCTA	Latitude	Longitude	Demand (kg)	ZCTA	Latitude	Longitude	Demand (kg)
97014	45.5829	−122.0168	4.50	97023	45.2785	−122.3232	3.75
97019	45.5156	−122.2427	4.00	97027	45.3856	−122.5928	4.50
97024	45.5466	−122.4424	3.25	97028	45.2884	−121.8074	4.75
97030	45.5092	−122.4336	1.75	97034	45.4094	−122.6835	1.50
97060	45.5313	−122.3691	2.75	97035	45.4135	−122.7252	2.75
97080	45.4783	−122.3907	3.75	97038	45.0954	−122.5590	2.25
97201	45.5079	−122.6908	2.00	97042	45.2052	−122.5398	4.25
97202	45.4827	−122.6444	4.50	97045	45.3203	−122.5365	2.25
97203	45.6035	−122.7379	4.75	97049	45.3464	−121.8624	2.25
97204	45.5184	−122.6739	2.25	97055	45.3888	−122.1552	1.25
97205	45.5206	−122.7102	3.25	97067	45.2978	−122.0544	3.25
97206	45.4824	−122.5986	3.75	97068	45.3523	−122.6686	5.00
97208	45.5287	−122.6790	3.25	97070	45.3061	−122.7731	2.25
97209	45.5311	−122.6839	2.25	97086	45.4452	−122.5281	5.00
97210	45.5442	−122.7267	4.75	97089	45.4266	−122.4431	3.00
97211	45.5811	−122.6373	4.25	97222	45.4409	−122.6181	1.25
97212	45.5442	−122.6435	3.50	97267	45.4084	−122.6129	2.00
97213	45.5382	−122.6000	1.25	98601	45.9434	−122.3625	1.75
97214	45.5147	−122.6430	2.50	98604	45.8057	−122.5108	4.00
97215	45.5151	−122.6006	2.75	98606	45.7297	−122.4564	3.75
97216	45.5139	−122.5584	2.75	98607	45.6422	−122.3800	3.00
97217	45.6018	−122.7008	1.75	98629	45.8766	−122.6192	1.75
97218	45.5763	−122.6009	3.25	98642	45.8077	−122.6939	1.75
97219	45.4542	−122.6985	1.25	98660	45.6790	−122.7205	1.50
97220	45.5500	−122.5593	3.25	98661	45.6401	−122.6250	3.75
97221	45.4983	−122.7288	2.50	98662	45.6885	−122.5778	3.00
97227	45.5434	−122.6781	4.50	98663	45.6574	−122.6632	3.00
97230	45.5578	−122.5053	1.25	98664	45.6195	−122.5772	4.00
97231	45.6876	−122.8242	3.25	98665	45.6795	−122.6606	1.50
97232	45.5289	−122.6439	3.50	98675	45.8285	−122.3429	2.50
97233	45.5151	−122.5033	2.00	98682	45.6732	−122.4817	4.50
97236	45.4829	−122.5098	5.00	98683	45.6033	−122.5102	3.25
97239	45.4924	−122.6925	3.25	98684	45.6306	−122.5148	4.00
97266	45.4830	−122.5582	5.00	98685	45.7152	−122.6931	4.75
97004	45.2550	−122.4494	4.75	98686	45.7234	−122.6244	1.25
97009	45.4230	−122.3328	1.75	97016	46.0603	−123.2670	1.75
97011	45.3871	−122.0264	1.25	97018	45.8971	−122.8106	2.75
97013	45.2208	−122.6683	2.00	97048	46.0448	−122.9820	2.75
97015	45.4135	−122.5368	1.25	97051	45.8793	−122.9500	3.75
97017	45.1765	−122.3897	1.50	97053	45.8280	−122.8833	2.75
97022	45.3467	−122.3200	2.25	97054	45.9422	−122.9496	1.25
97056	45.7720	−122.9694	4.50	97116	45.5808	−123.1657	2.00
97064	45.8591	−123.2355	4.00	97117	45.6314	−123.2884	3.00
97101	45.0902	−123.2287	4.25	97119	45.4689	−123.2002	3.25
97111	45.2845	−123.1952	3.75	97123	45.4402	−122.9801	2.75
97114	45.1879	−123.0766	3.75	97124	45.5698	−122.9496	2.25
97115	45.2752	−123.0395	3.50	97125	45.6711	−123.1969	1.75
97127	45.2461	−123.1114	4.25	97133	45.6861	−123.0227	3.50
97128	45.2119	−123.2822	4.25	97140	45.3531	−122.8659	4.50
97132	45.3242	−122.9873	5.00	97144	45.7416	−123.3002	2.25
97148	45.3584	−123.2485	3.75	97223	45.4403	−122.7766	3.75
97347	45.0771	−123.6564	1.50	97224	45.4055	−122.7951	1.75
97396	45.1040	−123.5490	3.75	97225	45.5016	−122.7700	2.00
97005	45.4910	−122.8036	3.25	97229	45.5510	−122.8093	2.00
97006	45.5170	−122.8598	3.25	98605	45.7769	−121.6655	4.25
97007	45.4543	−122.8796	2.00	98610	45.8659	−122.0652	4.75
97008	45.4602	−122.8042	2.25	98616	46.1933	−122.1329	4.75
97062	45.3693	−122.7623	1.75	98639	45.6699	−121.9897	1.75
97106	45.6657	−123.1190	3.75	98648	45.7063	−121.9563	2.75
97109	45.7378	−123.1812	3.00	98651	45.7399	−121.5835	3.50
97113	45.4972	−123.0443	1.50	98671	45.6144	−122.2384	1.50

Table A.8
List of all candidate facility locations.

ID	Latitude	Longitude	ID	Latitude	Longitude	ID	Latitude	Longitude
0	45.8169	−122.7459	35	45.4831	−122.8041	70	45.3608	−122.8451
1	45.8625	−122.6605	36	45.5167	−122.6071	71	45.4316	−122.7151
2	45.7812	−122.5273	37	45.5625	−122.6666	72	45.3535	−122.8665
3	45.6920	−122.5452	38	45.5986	−122.7853	73	45.4091	−122.7963
4	45.6610	−122.6360	39	45.5662	−122.6746	74	45.4824	−122.5887
5	45.6259	−122.5361	40	45.5502	−122.6619	75	45.4401	−122.8366
6	45.6335	−122.6613	41	45.5076	−122.4215	76	45.5074	−122.7971
7	45.6431	−122.6255	42	45.5206	−123.1042	77	45.5696	−122.6736
8	45.5820	−122.3905	43	45.5051	−122.4856	78	45.4682	−122.7100
9	45.5797	−122.3542	44	45.4266	−122.6061	79	45.4946	−122.6305
10	45.6923	−121.8941	45	45.4312	−122.5822	80	45.5085	−122.7179
11	45.7380	−121.5386	46	45.4771	−122.7040	81	45.1500	−122.5778
12	45.4682	−123.1438	47	45.4913	−122.6014	82	45.5199	−122.6246
13	45.5987	−122.9961	48	45.3036	−122.7586	83	45.5503	−122.6857
14	45.2993	−122.9750	49	45.3828	−122.7321	84	45.5422	−122.6649
15	45.3046	−122.9365	50	45.3863	−122.7670	85	45.4758	−122.7221
16	45.0740	−123.6141	51	45.3856	−122.7605	86	45.4487	−122.8064
17	45.2125	−123.1940	52	45.4233	−122.7685	87	45.5618	−122.6819
18	45.2432	−123.1160	53	45.5368	−122.4358	88	45.3549	−122.6060
19	45.2753	−123.0136	54	45.5212	−123.0579	89	45.5154	−122.9748
20	45.2191	−123.0760	55	45.5368	−122.8343	90	45.4710	−122.6790
21	45.0979	−123.3960	56	45.3968	−122.2691	91	45.5147	−122.9769
22	45.0765	−123.4832	57	45.4450	−122.7952	92	45.5278	−122.7097
23	46.1034	−123.2021	58	45.5290	−122.8065	93	45.5877	−122.7114
24	46.0933	−122.9440	59	45.2525	−122.6865	94	45.5158	−122.5532
25	45.8626	−122.8090	60	45.5987	−122.9961	95	45.5268	−122.5785
26	45.8459	−122.8259	61	45.3525	−122.5980	96	45.4648	−122.6513
27	45.5372	−122.2658	62	45.3816	−122.5923	97	45.5922	−122.7522
28	45.2852	−122.3368	63	45.4461	−122.6192	98	45.4798	−122.6188
29	45.0424	−122.6677	64	45.2852	−122.3368	99	45.4262	−122.6679
30	45.1499	−122.5777	65	45.3838	−122.5976	100	45.3699	−122.6488
31	45.5346	−122.6247	66	45.5976	−123.0012	101	45.4798	−122.8040
32	45.5708	−122.6097	67	45.5623	−122.6676	102	45.5396	−122.9626
33	45.5537	−122.6759	68	45.4666	−122.7535	103	45.3102	−122.7982
34	45.5339	−122.6854	69	45.5229	−122.9820			

Appendix B. Supplementary material

Supplementary data associated with this article can be found, in the online version, at https://doi.org/10.1016/j.trc.2018.12.001.

References

Agatz, N., Bouman, P., Schmidt, M., 2018. Optimization approaches for the traveling salesman problem with drone. Transp. Sci.

Albareda-Sambola, M., Fernández, E., Laporte, G., 2009. The capacity and distance constrained plant location problem. Comput. Oper. Res. 36 (2), 597–611.

Albornoz, C., Giraldo, L.F., 2017. Trajectory design for efficient crop irrigation with a uav. In: 2017 IEEE 3rd Colombian Conference on Automatic Control (CCAC). IEEE, pp. 1–6.

Amazon, 2018. Amazon prime air. https://www.amazon.com/Amazon-Prime-Air/b?ie=UTF8&node=8037720011 (accessed: May 2018).

Amicell, 2018. Li-polymer batteries. http://www.amicell.co.il/batteries/rechargeable-batteries/li-polymer-batteries/ (accessed: May 2018).

Amukele, T., Ness, P.M., Tobian, A.A., Boyd, J., Street, J., 2017. Drone transportation of blood products. Transfusion 57 (3), 582–588.

Anaya-Arenas, A.M., Renaud, J., Ruiz, A., 2014. Relief distribution networks: a systematic review. Ann. Oper. Res. 223 (1), 53–79.

Berner, B., Chojnacki, J., 2017. Use of drones in crop protection. In: IX International Scientific Symposium “Farm Machinery and Processes Management in Sustainable Agriculture”. IEEE, pp. 46–51.

Boutilier, J.J., Brooks, S.C., Janmohamed, A., Byers, A., Buick, J.E., Zhan, C., Schoellig, A.P., Cheskes, S., Morrison, L.J., Chan, T.C., 2017. Optimizing a drone network to deliver automated external defibrillators. Circulation 2454–2465.

Burema, H., Filin, A., 2016. Aerial farm robot system for crop dusting, planting, fertilizing and other field jobs. US Patent 9,382,003.

Carlsson, J.G., Song, S., 2017. Coordinated logistics with a truck and a drone. Manage. Sci.

Choi, Y., Schonfeld, P.M., 2017. Optimization of multi-package drone deliveries considering battery capacity. In: 96th Annual Meeting of the Transportation Research Board, Washington, DC (Paper No. 17-05769).

Chowdhury, S., Emelogu, A., Marufuzzaman, M., Nurre, S.G., Bian, L., 2017. Drones for disaster response and relief operations: a continuous approximation model. Int. J. Prod. Econ. 188, 167–184.

Church, R., ReVelle, C., 1974. The Maximal Covering Location Problem. In: Springer, pp. 101–118.

Claesson, A., Bäckman, A., Ringh, M., Svensson, L., Nordberg, P., Djärv, T., Hollenberg, J., 2017. Time to delivery of an automated external defibrillator using a drone for simulated out-of-hospital cardiac arrests vs emergency medical services. Jama 317 (22), 2332–2334.

Costa, F.G., Ueyama, J., Braun, T., Pessin, G., Osório, F.S., Vargas, P.A., 2012. The use of unmanned aerial vehicles and wireless sensor network in agricultural applications. In: Geoscience and Remote Sensing Symposium (IGARSS), 2012 IEEE International. IEEE, pp. 5045–5048.
Daknama, R., Kraus, E., 2017. Vehicle routing with drones. eprint arXiv:1705.06431. https://arxiv.org/pdf/1705.06431.pdf.
Daskin, M.S., 2011. Network and Discrete Location: Models, Algorithms, and Applications. John Wiley & Sons.
Dayarian, I., Savelsbergh, M., Clarke, J.-P., 2017. Same-day delivery with drone resupply. Optimization online. http://www.optimization-online.org/DB_FILE/2017/09/6206.pdf.
DHL, 2014. Unmanned aerial vehicles in logistics: a dhl perspective on implications and use for the logistics industry. http://www.dhl.com/content/dam/downloads/g0/about_us/logistics_insights/DHL_TrendReport_UAV.pdf (accessed: May 2018).
Dorling, K., Heinrichs, J., Messier, G.G., Magierowski, S., 2017. Vehicle routing problems for drone delivery. IEEE Trans. Syst., Man, Cybernet.: Syst. 47 (1), 70–85.
FAA, 2018a. Airspace restrictions. https://www.faa.gov/uas/where_to_fly/airspace_restrictions/ (accessed: Dec 2018).
FAA, 2018b. Faa begins drone airspace authorization expansion. https://www.faa.gov/news/updates/?newsId=90245 (accessed: May 2018).
Faiçal, B.S., Costa, F.G., Pessin, G., Ueyama, J., Freitas, H., Colombo, A., Fini, P.H., Villas, L., Osório, F.S., Vargas, P.A., et al., 2014. The use of unmanned aerial vehicles and wireless sensor networks for spraying pesticides. J. Syst. Architect. 60 (4), 393–404.
Farahani, R.Z., Asgari, N., Heidari, N., Hosseininia, M., Goh, M., 2012. Covering problems in facility location: a review. Comput. Ind. Eng. 62 (1), 368–407.
Fehrenbacher, K., 2018. A new lithium-metal battery takes flight in drones. https://www.greentechmedia.com/articles/read/a-new-lithium-metal-battery-takes-flight-in-drones#gs.s_bKMvI (accessed: May 2018).
Figliozzi, M., 2017. Lifecycle modeling and assessment of unmanned aerial vehicles (Drones) CO2e emissions. Transp. Res. Part D 57, 251–261.
Giles, D.K., Billing, R., Singh, W., 2016. Performance results, economic viability and outlook for remotely piloted aircraft for agricultural spraying. Aspects Appl. Biol. 132, 15–21.
Golabi, M., Shavarani, S.M., Izbirak, G., 2017. An edge-based stochastic facility location problem in uav-supported humanitarian relief logistics: a case study of tehran earthquake. Nat. Hazards 87 (3), 1545–1565.
Goodchild, A., Toy, J., 2017. Delivery by drone: An evaluation of unmanned aerial vehicle technology in reducing co2 emissions in the delivery service industry. Transp. Res. Part D: Transp. Environ.
Goundan, P.R., Schulz, A.S., 2007. Revisiting the greedy approach to submodular set function maximization. Optimization online. http://www.optimization-online.org/DB_FILE/2007/08/1740.pdf.
Ha, Q.M., Deville, Y., Pham, Q.D., Hà, M.H., 2018. On the min-cost traveling salesman problem with drone. Transp. Res. Part C: Emerg. Technol. 86, 597–621.
Halper, R., Raghavan, S., Sahin, M., 2015. Local search heuristics for the mobile facility location problem. Comput. Oper. Res. 62, 210–223.
Hassanalian, M., Abdelkefi, A., 2017. Classifications, applications, and design challenges of drones: a review. Prog. Aerosp. Sci. 99, 99–131.
Holguín-Veras, J., Jaller, M., Van Wassenhove, L.N., Pérez, N., Wachtendorf, T., 2012. On the unique features of post-disaster humanitarian logistics. J. Oper. Manage. 30 (7–8), 494–506.
Hong, I., Kuby, M., Murray, A.T., 2018. A range-restricted recharging station coverage model for drone delivery service planning. Transp. Res. Part C: Emerg. Technol. 90, 198–212.
Jain, K., Vazirani, V.V., 2001. Approximation algorithms for metric facility location and k-median problems using the primal-dual schema and Lagrangian relaxation. J. ACM (JACM) 48 (2), 274–296.
Kang, J., Park, S., 2003. Algorithms for the variable sized bin packing problem. Eur. J. Oper. Res. 147 (2), 365–372.
Karaca, Y., Cicek, M., Tatli, O., Sahin, A., Pasli, S., Beser, M.F., Turedi, S., 2018. The potential use of unmanned aircraft systems (drones) in mountain search and rescue operations. Am. J. Emerg. Med. 36, 585–588.
Kim, S.J., Lim, G.J., Cho, J., 2018. Drone flight scheduling under uncertainty on battery duration and air temperature. Comput. Ind. Eng. 117, 291–302.
Kim, S.J., Lim, G.J., Cho, J., Côté, M.J., 2017. Drone-aided healthcare services for patients with chronic diseases in rural areas. J. Intell. Robot. Syst. 88 (1), 163–180.
Li, K.-R., See, K.-Y., Koh, W.-J., Zhang, J.-W., 2017. Design of 2.45 GHz microwave wireless power transfer system for battery charging applications. In: Progress in Electromagnetics Research Symposium-Fall (PIERS-FALL). IEEE, pp. 2417–2423.
Loulou, R., Michaelides, E., 1979. New greedy-like heuristics for the multidimensional 0-1 knapsack problem. Oper. Res. 27 (6), 1101–1114.
Mack, E., 2018. How delivery drones can help save the world. https://www.forbes.com/sites/ericmack/2018/02/13/delivery-drones-amazon-energy-efficient-reduce-climate-change-pollution/#476a63f56a87 (accessed: May 2018).
Melo, M.T., Nickel, S., Saldanha-Da-Gama, F., 2009. Facility location and supply chain management–a review. Eur. J. Oper. Res. 196 (2), 401–412.
Microdrones, 2018. The heavy lifting drone - md4300. https://www.amazon.com/Amazon-Prime-Air/b?ie=UTF8&node=8037720011 (accessed: May 2018).
Murray, C.C., Chu, A.G., 2015. The flying sidekick traveling salesman problem: optimization of drone-assisted parcel delivery. Transp. Res. Part C: Emerg. Technol. 54, 86–109.
Otto, A., Agatz, N., Campbell, J., Golden, B., Pesch, E., 2018. Optimization approaches for civil applications of unmanned aerial vehicles (uavs) or aerial drones: a survey. Networks. https://doi.org/10.1002/net.21818.
Ozdamar, L., 2011. Planning helicopter logistics in disaster relief. OR Spectrum 33 (3), 655–672.
Pirkul, H., Schilling, D., 1989. The capacitated maximal covering location problem with backup service. Ann. Oper. Res. 18 (1), 141–154.
Poikonen, S., Wang, X., Golden, B., 2017. The vehicle routing problem with drones: extended models and connections. Networks 70 (1), 34–43.
Ponza, A., 2016. Optimization of Drone-assisted Parcel Delivery (Master's thesis). University of Padova.
Puchinger, J., Raidl, G.R., 2007. Models and algorithms for three-stage two-dimensional bin packing. Eur. J. Oper. Res. 183 (3), 1304–1327.
Pulver, A., Wei, R., 2018. Optimizing the spatial location of medical drones. Appl. Geogr. 90, 9–16.
Scott, J.E., Scott, C.H., 2018. Models for drone delivery of medications and other healthcare items. Int. J. Healthcare Inform. Syst. Inform. (IJHISI) 13 (3), 20–34.
Shmoys, D.B., Tardos, É., Aardal, K., 1997. Approximation algorithms for facility location problems. In: Proceedings of the Twenty-ninth Annual ACM Symposium on Theory of Computing. ACM, pp. 265–274.
Thiels, C., Aho, J., Zietlow, S., Jenkins, D., 2015. Use of unmanned aerial vehicles for medical product transport. Air Med. J. 34 (2), 104–108.
Wang, C., He, X., Liu, Y., Song, J., Zeng, A., 2016. The small single and multirotor unmanned aircraft vehicles chemical application techniques and control for rice fields in china. Aspects Appl. Biol. 132, 73–81.
Wang, X., Poikonen, S., Golden, B., 2017. The vehicle routing problem with drones: several worst-case results. Optim. Lett. 11 (4), 679–697.
Wu, T.-H., Low, C., Bai, J.-W., 2002. Heuristic solutions to multi-depot location-routing problems. Comput. Oper. Res. 29 (10), 1393–1415.
Yanmaz, E., Quaritsch, M., Yahyanejad, S., Rinner, B., Hellwagner, H., Bettstetter, C., 2017. Communication and coordination for drone networks. In: Ad Hoc Netwrks. Springer, pp. 79–91.
Yanmaz, E., Yahyanejad, S., Rinner, B., Hellwagner, H., Bettstetter, C., 2018. Drone networks: communications, coordination, and sensing. Ad Hoc Netw. 68, 1–15.
Yurek, E.E., Ozmutlu, H.C., 2018. A decomposition-based iterative optimization algorithm for traveling salesman problem with drone. Transp. Res. Part C: Emerg. Technol. 91, 249–262.